Application of variational method for three-color three-photon transitions in hydrogen atom implanted in Debye plasmas

S. Paul[a] and Y. K. Ho
Institute of Atomic and Molecular Sciences, Academia Sinica, P.O. Box 23-166, Taipei, Taiwan 106, Republic of China

(Received 27 August 2009; accepted 15 October 2009; published online 11 November 2009)

Multiphoton processes, where transparency appears, have long fascinated physicists. Plasma screening effects are investigated on three-color three-photon bound-bound transitions in hydrogen atom embedded in Debye plasmas; where photons are linearly and circularly polarized, two left circular and one right circular. All possible combinations of frequency and polarization are considered. Analytical wave functions are used for initial and final states along with the pseudostate wave functions for intermediate states. The analytical wave functions are obtained from the modified wave functions for screening Coulomb potential (Debye model) using Ritz variational method. Here, we have found three-photon transparency for lower values of Debye length. This type of phenomenon occurs due to energy level shifting in the presence of Debye plasma environments. The description of resonance enhancements and three-photon transparency is reported in the present context along with the region of resonance enhancements and three-photon transparency. © *2009 American Institute of Physics*. [doi:10.1063/1.3258665]

I. INTRODUCTION

Currently, there is a rapid growth in both experimental and theoretical studies of multiphoton processes and multiphoton spectroscopy of atoms, ions, and molecules in chemistry, physics, biology, material science, etc., for a collection of review papers in these areas we refer to the book edited by Lin *et al.*,[1] where a comprehensive bibliography can be found. Nonlinear optical method such as two-photon and three-photon absorption are powerful tools to investigate electronic properties. Because of additional degree of freedom in experiments, where more than one photon is participating in an elementary absorption process, one expects additional information as compared to one-photon absorption. Due to different selection rules new electronic resonances can be excited.

Plasma physics plays an enormous role both in the natural world and in the world of technology. We use plasmas for lighting (candle flames, campfires, fluorescent lights, sodium vapor lights, etc.), industrial processing (microchips, studies of chemical reactions, etc.), fusion energy research and neutron production, x-ray lasers, etc. Presently, considerable interest has been cultivated in the study of atomic processes in plasma environments[2–18] because of the plasma screening effect on the plasma-embedded atomic systems. A number of studies have been conducted on the investigation of the influence of plasma on scattering processes. The screening effects have played a crucial and significant part in the investigation of plasma environments over the past several decades. Different theoretical methods have been employed along with the Debye screening to study plasma environments.[12–29] Debye plasma is considered here, the concept of the Debye screening is valid only in a steady, thermodynamical equilibrium, and linear plasma.

[a]Electronic mail: spaul@pub.iams.sinica.edu.tw.

The hydrogen atom has special significance in quantum mechanics and quantum field theory as a simple two-body problem physical system which has yielded analytical solution in closed form. Many surveys have been conducted on the simplest atom, resulting in the vast accumulation of data and reports which have been systematically arranged and well documented in the literature. In the present context, linearly and circularly polarized three-color three-photon spectroscopy of the $1s$-$2p$ transition in hydrogen atom (free and immersed in Debye plasmas) is studied theoretically for the first time, to our knowledge.

The Hamiltonian of a hydrogen atom surrounded by Debye plasmas in atomic unit is

$$H = -\nabla^2 - \frac{1}{r}e^{-r/\lambda_D}, \tag{1}$$

where $-(1/r)e^{-r/\lambda_D}$ is the Debye screening potential for a hydrogen atom with λ_D being the Debye screening length.

II. THEORY

Our goal is to calculate transition amplitudes of hydrogen atom in Debye plasma environment. For our present study, we have considered variational method for initial and final states and adopted pseudostate summation technique for intermediate states. Below we show the entire analytical calculation of the current context by three subsections.

A. Linearly polarized three-color three-photon

The purpose of the work is a study of the excitation of ground state atomic hydrogen, by simultaneous absorption of three photons of frequencies ω_1, ω_2, and ω_3. Here, all the possible values of ω_1, ω_2, and ω_3 are considered. Six Feynman diagrams (Fig. 1) of third order are associated with the

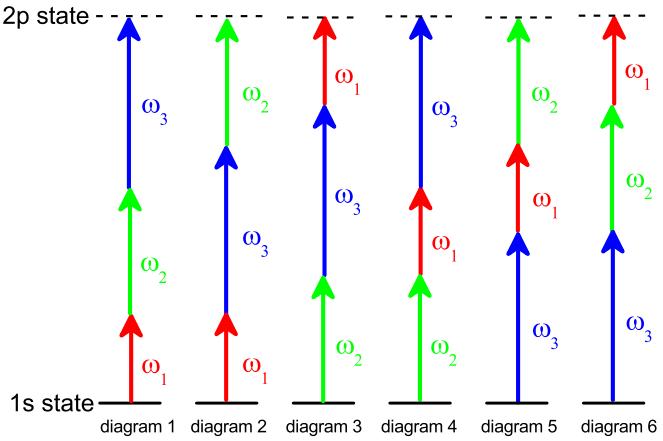

FIG. 1. (Color online) Feynman diagrams associated with the process of excitation of the hydrogen atom initially in the ground state, by three-photon absorption, all of the different frequency.

process in which three photons are absorbed. In the dipole approximation, the amplitude of the process is constructed using a third-order tensor as follows:

$$M = \tfrac{1}{6}[\Pi_{\omega_1\omega_2\omega_3}(\Omega_1,\Omega'_{12}) + \Pi_{\omega_1\omega_3\omega_2}(\Omega_1,\Omega'_{13}) + \Pi_{\omega_2\omega_3\omega_1}(\Omega_2,\Omega'_{23}) + \Pi_{\omega_2\omega_1\omega_3}(\Omega_2,\Omega'_{21}) + \Pi_{\omega_3\omega_1\omega_2}(\Omega_3,\Omega'_{31}) + \Pi_{\omega_3\omega_2\omega_1}(\Omega_3,\Omega'_{32})], \quad (2)$$

where

$$\Pi_{\omega_j\omega_k\omega_l} = \sum_{n,n'} \frac{\langle f|\vec{\epsilon}_j\cdot\vec{r}|n\rangle\langle n|\vec{\epsilon}_k\cdot\vec{r}|n'\rangle\langle n'|\vec{\epsilon}_l\cdot\vec{r}|i\rangle}{(E_n-\Omega'_{jk})(E_{n'}-\Omega_j)}, \quad (3)$$

(j,k,*l*) corresponds to the six permutations (1, 2, 3), (1, 3, 2), (2, 3, 1), (2, 1, 3), (3, 1, 2), and (3, 2, 1) for three different frequencies. Here, $\vec{\epsilon}_j$ is the unit polarization vector of the incident radiation field with frequency ω_j. From energy conservation, we have $E_f - E_i = \hbar\omega_1 + \hbar\omega_2 + \hbar\omega_3$, where E_i and E_f are energies of initial state $|i\rangle$ and final state $|f\rangle$, respectively. In the above expression, $|n\rangle$ and $|n'\rangle$ are intermediate states and E_n, $E_{n'}$ are corresponding energies. The parameters Ω_j and Ω'_{jk} corresponding to the six Feynman diagrams in Fig. 1 are

$$\Omega_j = E_i + \hbar\omega_j, \quad \Omega'_{jk} = E_i + \hbar\omega_j + \hbar\omega_k. \quad (4)$$

For simplicity, we consider all three photons are linearly polarized, i.e., $\vec{\epsilon}_j = \vec{\epsilon}_k = \vec{\epsilon}_l = \vec{\epsilon}$. Therefore, the expression (3) reduces to an elementary form, given below,

$$\Pi_{\omega_j\omega_k\omega_l} = \sum_{n,n'} \frac{C_{nn'}}{(E_n-\Omega'_{jk})(E_{n'}-\Omega_j)}, \quad (5)$$

where

$$C_{nn'} = \langle f|\vec{\epsilon}\cdot\vec{r}|n\rangle\langle n|\vec{\epsilon}\cdot\vec{r}|n'\rangle\langle n'|\vec{\epsilon}\cdot\vec{r}|i\rangle. \quad (6)$$

Here we consider linear polarization, so

$$\vec{\epsilon}\cdot\vec{r} = \left(\tfrac{4}{3}\pi\right)^{1/2} r Y_{10}(\hat{r}). \quad (7)$$

There are two available angular momentum channels for three-photon 1*s*-2*p* transition, one is *s*-*p*-*s*-*p* channel and the second is *s*-*p*-*d*-*p* channel. The expressions of $C_{nn'}$ for different channels are varied as given below: for *s*-*p*-*s*-*p* channel,

$$C_{nn'} = \frac{1}{3\sqrt{3}}\langle \Re_{2p}|r|R_{ns}\rangle\langle R_{ns}|r|R_{n'p}\rangle\langle R_{n'p}|r|\Re_{1s}\rangle, \quad (8)$$

and for *s*-*p*-*d*-*p* channel,

$$C_{nn'} = \frac{4}{15\sqrt{3}}\langle \Re_{2p}|r|R_{nd}\rangle\langle R_{nd}|r|R_{n'p}\rangle\langle R_{n'p}|r|\Re_{1s}\rangle. \quad (9)$$

We consider variation method for initial and final states and pseudostate summation technique for intermediate states, which includes both discrete and continuum. $\Re_{1s}$, $\Re_{2p}$ are radial part of the variational wave functions [Eq. (2) in Ref. 30] and R_{np}, $R_{n's}$, $R_{n'd}$ are radial part of the pseudostate wave function [Eq. (3) in Ref. 27]. We denote $D^{(3)L}_{1s\text{-}p\text{-}s\text{-}2p}$ and $D^{(3)L}_{1s\text{-}p\text{-}d\text{-}2p}$ as the transition amplitudes for 1*s*-2*p* transitions followed by *s*-*p*-*s*-*p* channel and *s*-*p*-*d*-*p* channel, respectively. Again we consider

$$D^{(3)L}_{1s\text{-}2p} = D^{(3)L}_{1s\text{-}p\text{-}s\text{-}2p} + D^{(3)L}_{1s\text{-}p\text{-}d\text{-}2p}, \quad (10)$$

where $D^{(3)L}_{1s\text{-}2\text{-}p}$ are the transition amplitudes for 1*s*-2*p* transition. *L* indicates linearly polarized photons.

B. Circularly polarized three-color three-photon

Here, we study 1*s*-2*p* transition in hydrogen atom, by simultaneous absorption of three photons γ_1, γ_2, and γ_3 of frequencies ω_1, ω_2, and ω_3. The orientations of three photons γ_1, γ_2, and γ_3 are left circular, right circular, and left circular, respectively. Here all possible values of ω_1, ω_2, and ω_3 are considered. We regard circular polarization, two photons are left circular and one is right circular. The process of two left and one right circular polarized photons is equivalent to the process of two right and one left circular polarized photons. There are two available angular momentum channels for three-photon 1*s*-2*p* transition, one is *s*-*p*-*s*-*p* channel and the second is *s*-*p*-*d*-*p* channel. All possible combinations of polarization and frequency are presented in Fig. 2 along with corresponding Feynman diagrams. There are three possible combinations of circular polarization, these are left-right-left (LRL), right-left-left (RLL), and left-left-right (LLR). Selection rule indicates that LLR circular polarization arrangement is impossible for *s*-*p*-*s*-*p* channel. In the dipole approximation, the amplitude of the general process is constructed using a third-order tensor, followed by the Feynman diagrams (Fig. 2), as follows:

$$M = \frac{1}{n_p}[\Pi^{\mathrm{LRL}}_{\omega_1\omega_2\omega_3} + \Pi^{\mathrm{LRL}}_{\omega_3\omega_2\omega_1} + \Pi^{\mathrm{RLL}}_{\omega_2\omega_1\omega_3} + \Pi^{\mathrm{RLL}}_{\omega_2\omega_3\omega_1} + \Pi^{\mathrm{LLR}}_{\omega_1\omega_3\omega_2} + \Pi^{\mathrm{LLR}}_{\omega_3\omega_1\omega_2}], \quad (11)$$

where superscripts denote sequence of circular polarization (left and right) and n_p is the total number of possibilities. Here

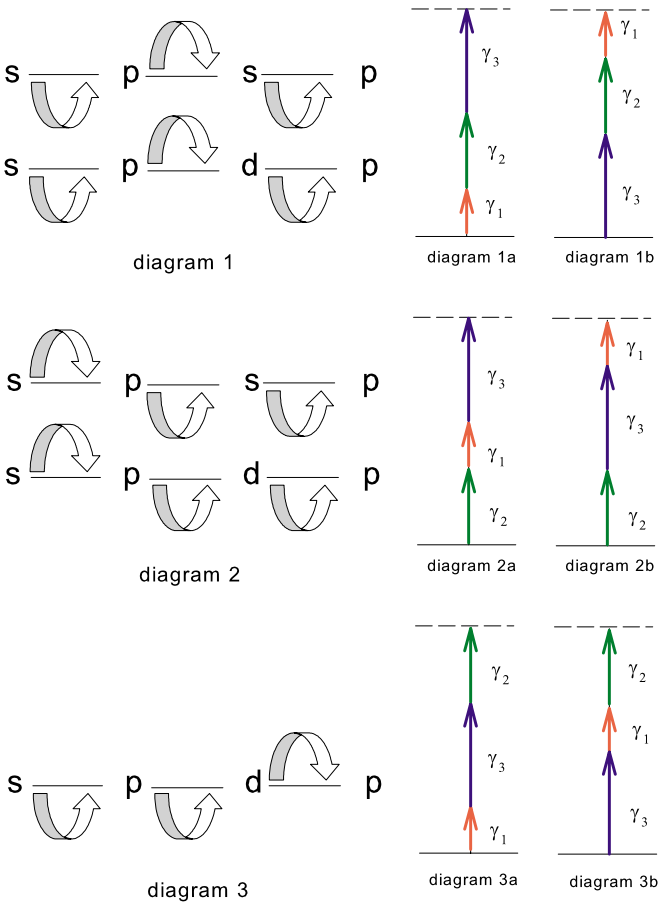

FIG. 2. (Color online) Combinations of circular polarizations (left side of the figure) and corresponding Feynman diagrams (right side of the figure), associated with the process of excitation of the hydrogen atom by absorption of three photons. Arrangement: diagram 1, left-right-left; diagram 2, right-left-left; diagram 3, left-left-right. γ_1, γ_2, and γ_3 are three photons of frequencies ω_1, ω_2, and ω_3 and polarization left circular, right circular, and left circular, respectively.

$$\Pi^{IJK}_{\omega_i\omega_j\omega_k} = \sum_{n,n'} \frac{\langle f|\vec{\epsilon}_I\cdot\vec{r}|n\rangle\langle n|\vec{\epsilon}_J\cdot\vec{r}|n'\rangle\langle n'|\vec{\epsilon}_K\cdot\vec{r}|g\rangle}{(E_n-\Omega'_{ij})(E_{n'}-\Omega_i)}, \tag{12}$$

where $\vec{\epsilon}_I$ is the unit polarization vector of the incident radiation field with frequency ω_i. I is either L or R corresponding to left and right circular polarization. From energy conservation, we have $\Delta E=E_f-E_g=\hbar\omega_1+\hbar\omega_2+\hbar\omega_3$, where E_g and E_f are energies of the initial state $|g\rangle$ and the final state $|f\rangle$, respectively. In the above expression, $|n\rangle$ and $|n'\rangle$ are intermediate states and E_n, $E_{n'}$ are the corresponding energies. The parameters Ω_i and Ω'_{ij} corresponding to the six Feynman diagrams in Fig. 2 are

$$\Omega_i = E_g+\hbar\omega_i, \quad \Omega'_{ij} = E_g+\hbar\omega_i+\hbar\omega_j. \tag{13}$$

Here we consider circular polarization, so

$$\vec{\epsilon}_I\cdot\vec{r} = \left(\tfrac{4}{3}\pi\right)^{1/2} r Y_{1\mu_I}(\hat{r}), \tag{14}$$

where $\mu_I=1$ for left circular polarization ($I=L$) and $\mu_I=-1$ for right circular polarization ($I=R$). After evaluating the angular integrations, Eq. (12) reduces to an elementary form, given below,

$$\Pi^{IJK}_{\omega_i\omega_j\omega_k} = F_{IJK}\sum_{n,n'} \frac{C_{nn'}}{(E_n-\Omega'_{ij})(E_{n'}-\Omega_i)}, \tag{15}$$

where F_{IJK} is the angular integration factor and

$$C_{nn'} = \langle R_f|r|R_n\rangle\langle R_n|r|R'_n\rangle\langle R'_n|r|R_g\rangle. \tag{16}$$

In the above expression, R_g and R_f are radial parts of the initial and final state wave functions, respectively, and R_n, $R_{n'}$ are that of intermediate states. Analytical wave functions are used for initial and final states; for screening Coulomb potential (Debye model), we use modified wave function[29] based on Ritz variation method. R_n and $R_{n'}$ are calculated by using pseudostate summation technique[30] with basis size of 30. The factor F_{IJK} is the product of three angular integration, express as

$$F_{IJK} = \left(\frac{4\pi}{3}\right)^{3/2}\langle Y_{l_1m_1}|Y_{1\mu_I}|Y_{l_2m_2}\rangle\times\langle Y_{l_2m_2}|Y_{1\mu_J}|Y_{l_3m_3}\rangle \times\langle Y_{l_3m_3}|Y_{1\mu_K}|Y_{l_4m_4}\rangle, \tag{17}$$

where $\mu_N=+1$, $\Delta l=\pm 1$, $\Delta m=+1$ for left circular polarization and $\mu_N=-1$, $\Delta l=\pm 1$, $\Delta m=-1$ for right circular polarization. We denote $D^{(3)C}_{1s\text{-}p\text{-}s\text{-}2p}$ and $D^{(3)C}_{1s\text{-}p\text{-}d\text{-}2p}$ as the transition amplitudes for $1s$-$2p$ transitions followed by s-p-s-p channel and s-p-d-p channel, respectively. The expressions of $D^{(3)C}_{1s\text{-}p\text{-}s\text{-}2p}$ and $D^{(3)C}_{1s\text{-}p\text{-}d\text{-}2p}$ are given below,

$$D^{(3)C}_{1s\text{-}p\text{-}s\text{-}2p} = -\tfrac{1}{4}[\Pi^{\mathrm{LRL}}_{\omega_1\omega_2\omega_3}+\Pi^{\mathrm{LRL}}_{\omega_3\omega_2\omega_1}+\Pi^{\mathrm{RLL}}_{\omega_2\omega_1\omega_3}+\Pi^{\mathrm{RLL}}_{\omega_2\omega_3\omega_1}], \tag{18}$$

$$D^{(3)C}_{1s\text{-}p\text{-}d\text{-}2p} = -\tfrac{1}{6}[\Pi^{\mathrm{LRL}}_{\omega_1\omega_2\omega_3}+\Pi^{\mathrm{LRL}}_{\omega_3\omega_2\omega_1}+\Pi^{\mathrm{RLL}}_{\omega_2\omega_1\omega_3}+\Pi^{\mathrm{RLL}}_{\omega_2\omega_3\omega_1} +\Pi^{\mathrm{LLR}}_{\omega_1\omega_3\omega_2}\Pi^{\mathrm{LLR}}_{\omega_3\omega_1\omega_2}]. \tag{19}$$

Again we consider

$$D^{(3)C}_{1s-2p} = D^{(3)C}_{1s\text{-}p\text{-}s\text{-}2p}+D^{(3)C}_{1s\text{-}p\text{-}d\text{-}2p}, \tag{20}$$

where $D^{(3)C}_{1s\text{-}2p}$ are the transition amplitudes for $1s$-$2p$ transition. C indicates circularly polarized photons.

C. Method

We calculate the initial ($1s$) and final ($2p$) states by variation method, a short description of the approach is presented here (for detail, see Ref. 29). The radial Schrödinger equation for hydrogen atom in dense plasma would be given by

$$\left\{-\frac{\hbar^2}{2m}\left[\frac{d^2}{dr^2}-\frac{l(l+1)}{r^2}\right]-\frac{Ze^2}{r}e^{-r/\lambda_D}\right\}P_{nl}(r) = E_{nl}P_{nl}, \tag{21}$$

where $P_{nl}(r)$ is the radial wave function for the nlth shell. The numerical solutions and higher order perturbation calculation have been evaluated for Eq. (21). Here we shall consider a simple analytical method to obtain the solution. Our approach is the same as the procedure of Jung[12] but in a more general way. Jung has calculated for the $1s$, $2s$, and $2p$ states only. The solutions for Eq. (21) are assumed to be in the hydrogenic form with a variation parameter. The trial wave function is considered, as follows:

$$P_{nl}(r) \equiv rR_{nl}(r) = \frac{1}{n}\left[\frac{(n-l-1)!}{\alpha(n+l)!}\right]^{1/2}\left(\frac{2r}{n\alpha}\right)^{l+1} L_{n-l-1}^{2l+1}\left(\frac{2r}{n\alpha}\right)e^{-r/n\alpha}, \quad (22)$$

where α is the variational parameter and

$$\alpha \to a_z \quad \text{for } \lambda_D \to \infty, \quad (23)$$

$a_z = a_0/z$, a_0 is Bohr radius, and $\lambda_D \to \infty$ indicates plasma free situation. L_{n-l-1}^{2l+1} is the usual Laguerre polynomial. Substitute the expression of trial wave function into the Schrödinger equation, we get

$$\langle E_{nl}\rangle = -\frac{\hbar^2}{2m}\left[\frac{1}{n^2\alpha^2} - \frac{2}{\alpha}\int_0^\infty P_{nl}(r)\frac{1}{r}P_{nl}(r)dr\right] - Ze^2\int_0^\infty P_{nl}(r)\frac{1}{r}e^{-r/\lambda_D}P_{nl}(r)dr. \quad (24)$$

After evaluating the integrations and simplification, we have

$$\langle E_{nl}\rangle = \frac{\hbar^2}{2m}\frac{1}{n^2\alpha^2} - \frac{Ze^2}{n^2\alpha}\cdot\frac{1}{\left(1+\frac{n\alpha}{2\lambda_D}\right)^{2n}} \times \sum_{k=0}^{n-l-1}\binom{n+l}{k}\binom{n-l-1}{k}\left(\frac{n\alpha}{2\lambda_D}\right)^{2k}, \quad (25)$$

which is the expectation value of the nl state energy of hydrogen atom in plasmas. Equation (25) shows that the energy level of hydrogen atom in plasmas depends on both n (the principal quantum number) and l (the orbital quantum number). The parameter α is obtained from the minimization condition of $\langle E_{nl}\rangle$, i.e., $\partial/\partial\alpha\langle E_{nl}\rangle = 0$ which gives

$$\alpha = a_z\left(1+\frac{n\alpha}{2\lambda_D}\right)^{2n}\left[\frac{n^2\left(\frac{\alpha}{\lambda_D}\right)}{\left(1+\frac{n\alpha}{2\lambda_D}\right)}\sum_{k=0}^{n-l-1}A_k\left(\frac{n\alpha}{2\lambda_D}\right)^{2k} + \sum_{k=0}^{n-l-1}(1-2k)A_k\left(\frac{n\alpha}{2\lambda_D}\right)^{2k}\right]^{-1}, \quad (26)$$

where

$$A_k = \binom{n+l}{k}\binom{n-l-1}{k}. \quad (27)$$

The variational parameter α is calculated by fixed point iteration method with the initial condition $\alpha_0 = a_z$ [by the help of condition (23)]. We calculate the intermediate states by using the pseudostate summation method (for detail, see Refs. 28 and 29). The basis functions of the pseudostate method are taken of the form (Drachman *et al.*[30])

$$\phi_j = e^{-ar}r^{l+j}Y_{lm}(\theta,\phi), \quad j = 0,1,\ldots,N-1, \quad (28)$$

where a is the basis parameter, l is the orbital angular momentum, and N is the basis size. Here it should be noted that the parameter a is adjustable. We consider the values of the adjustable parameter $a=1$ for s-states, $a=0.5$ for p-states, and $a=0.3$ for d-states. The value of N is 30 in the present calculations.

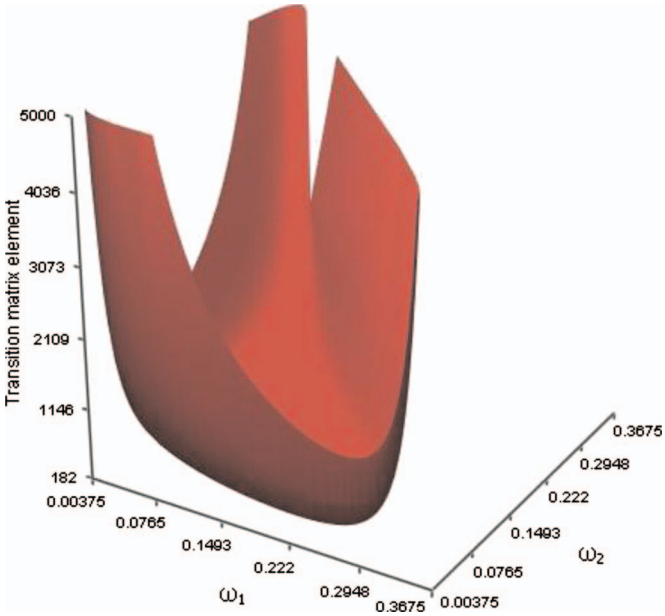

FIG. 3. (Color) Transition matrix elements $D_{1s\text{-}2p}^{(3)L}$ for $1s$-$2p$ transition in free hydrogen atom as a function of photon frequencies ω_1 and ω_2. L indicates linearly polarized photons.

The wave functions are expanded in terms of linear combinations of the basis functions as

$$\Psi_n = \sum_{j=0}^{N-1} C(j,n)\phi_j \quad (29)$$

and we have

$$\langle n|H|n'\rangle = E_n\Delta_{nn'}, \quad \langle n|n'\rangle = \Delta_{nn'}. \quad (30)$$

The finite-dimensional eigenvalue problem corresponding to the Hamiltonian of a hydrogen atom in plasmas field is the following:

$$(\underline{H} - E_n\underline{\Delta})|n\rangle = 0, \quad (31)$$

where $\underline{H}$ and $\underline{\Delta}$ are the Hamiltonian matrix and the overlap matrix, respectively (for more detailed see the Ref. 27).

III. RESULTS AND DISCUSSION

In the present section, we demonstrate some calculated data with a short description about resonance enhancement and three-photon transparency.

A. Linearly polarized photons

Figure 3 shows three-photon $1s$-$2p$ transition amplitudes for free hydrogen atom as a function of ω_1 and ω_2, the frequencies of photons. In Figs. 4 and 5, we observe the partial transition matrix elements due to the s-p-s-p and s-p-d-p channels, respectively. These figures show that the partial transition amplitudes of s-p-s-p channel dominate that of for s-p-d-p channel. In Figs. 3–5, we observe three resonance enhancements when the pair of frequencies (ω_1, ω_2),

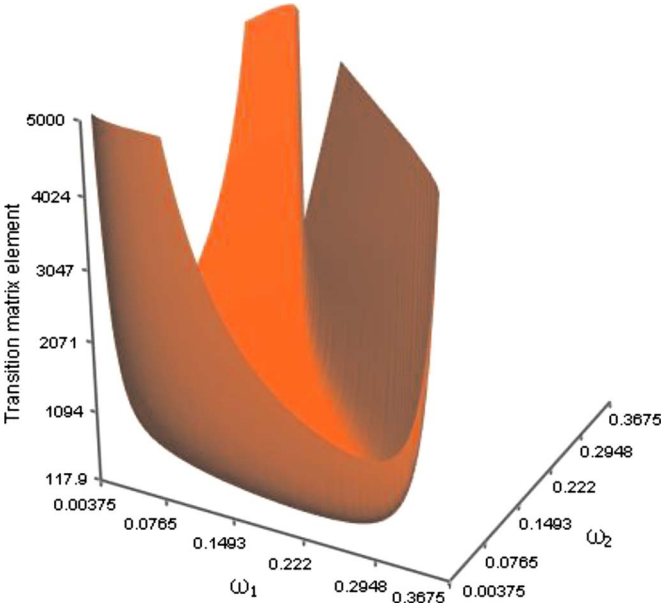

FIG. 4. (Color online) Partial transition matrix elements $D^{(3)L}_{1s\text{-}p\text{-}s\text{-}2p}$ for $1s$-$2p$ transition in free hydrogen atom as a function of photon frequencies ω_1 and ω_2. L indicates linearly polarized photons.

(ω_2, ω_3), and (ω_3, ω_1) each reaches minimum values. There is no three-photon transparency for free hydrogen. In the presence of Debye plasma field with Debye length of 7, we observe three-photon transparency (shown in Fig. 6) and resonance enhancements, similar to the free hydrogen case, when frequencies of two photons are very small. As free hydrogen case, the magnitudes of transition amplitude for the *s-p-s-p* channel (Fig. 7) are always greater than those of for *s-p-d-p* channel (Fig. 8). In Figs. 6 and 7, we observe some stripe in the curve surfaces. Those are no physical significance. To construct the prominent figures, the used software package automatically generates such type of ribbon. In the case of *s-p-d-p* channel transition amplitudes, there is no three-photon transparency. We calculate three-photon transition amplitudes for $\lambda_D=\infty$, 100, 50, 10, 9, 8, and 7. Three-photon transparency remains absent from large values of Debye length up to $\lambda_D=10$, for $\lambda=9$, three photon transparency is started to appear. The shapes of the curves for three-photon $1s$-$2p$ transition amplitudes are more or less the same for $\lambda_D=\infty$, 100, 50, and 10; only the bottom of the curves become flatter as λ_D decreasing. The diagrams of transition matrix elements for $\lambda_D=9$, 8, and 7 are similar. In Tables I and II, we report some numerical data of partial transition matrix elements $D^{(3)L}_{1s\text{-}p\text{-}s\text{-}2p}$ and $D^{(3)L}_{1s\text{-}p\text{-}d\text{-}2p}$ for $\lambda_D=\infty$ and λ_D

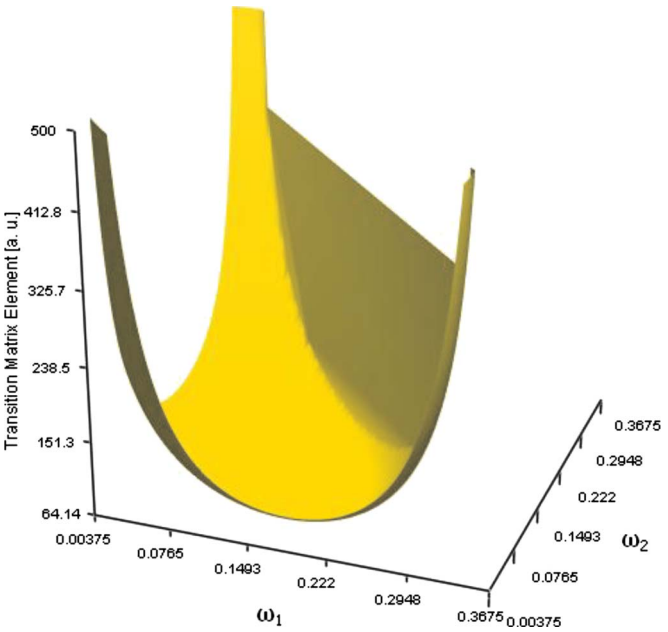

FIG. 5. (Color online) Partial transition matrix elements $D^{(3)L}_{1s\text{-}p\text{-}d\text{-}2p}$ for $1s$-$2p$ transition in free hydrogen atom as a function of photon frequencies ω_1 and ω_2. L indicates linearly polarized photons.

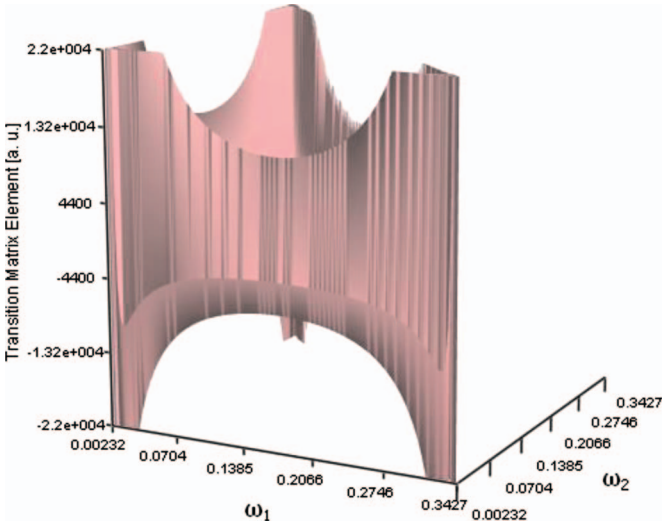

FIG. 6. (Color) Transition matrix elements $D^{(3)L}_{1s\text{-}2p}$ for $1s$-$2p$ transition in hydrogen atom embedded in Debye plasma with Debye length of 7 as a function of photon frequencies ω_1 and ω_2. L indicates linearly polarized photons.

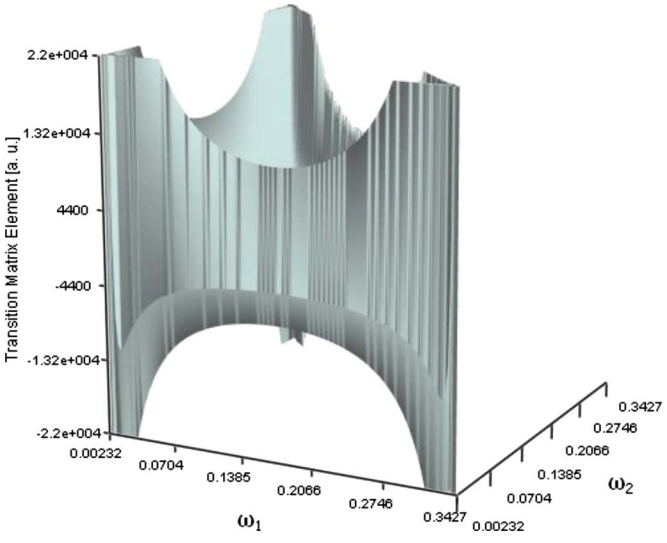

FIG. 7. (Color online) Partial transition matrix elements $D^{(3)L}_{1s\text{-}p\text{-}s\text{-}2p}$ for $1s$-$2p$ transition in hydrogen atom embedded in Debye plasma with Debye length of 7 as a function of photon frequencies ω_1 and ω_2. L indicates linearly polarized photons.

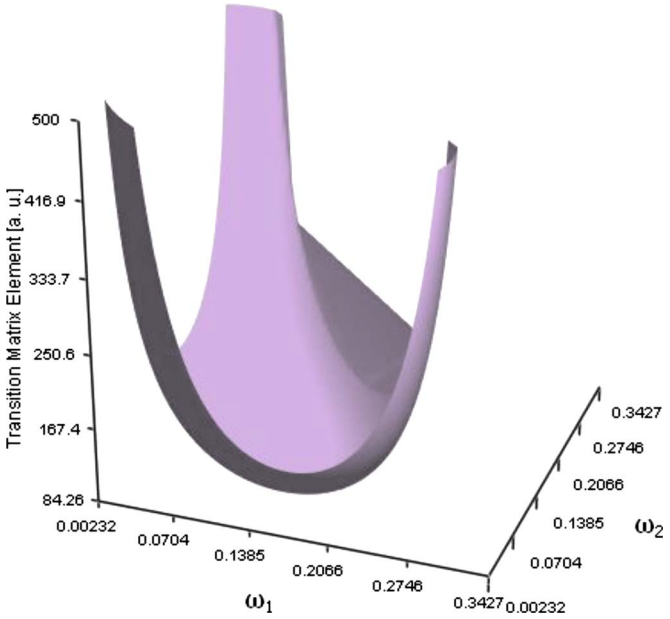

FIG. 8. (Color online) Partial transition matrix elements $D^{(3)L}_{1s\text{-}p\text{-}d\text{-}2p}$ for $1s$-$2p$ transition in hydrogen atom embedded in Debye plasma with Debye length of 7 as a function of photon frequencies ω_1 and ω_2. L indicates linearly polarized photons.

=7, respectively. Here, we present transition matrix elements for $\lambda_D=7$. The computed one-color three-photon transition amplitudes for $\omega_1=\omega_2=\omega_3$ agree excellently with the results of Thayyullathil *et al.*[31] and our earlier work.[29] In our pervious calculation[29] we used pseudostate summation method, the basis functions are different from the usual basis functions, to evaluate initial and final state wave functions.

1. Resonance enhancement

The process is said to be resonant whenever an intermediate state of the target spectrum is closely reached from the initial state by absorption of one or two photons. In the present section, we discuss about resonance enhancement for individual channel. From Eqs. (2), (4), and (5) the transition matrix element M can be expressed as

TABLE I. Linearly polarized three-photon transition amplitudes for free hydrogen atom as a function of incident photon frequencies in atomic unit.

ω_1	ω_2	$D^{(3)L}_{1s\text{-}p\text{-}s\text{-}2p}$	$D^{(3)L}_{1s\text{-}p\text{-}d\text{-}2p}$
0.045	0.3000	737.330 62	194.871 28
0.120	0.1500	122.556 03	65.392 57
0.150	0.1800	202.814 57	78.431 27
0.165	0.1500	161.793 66	72.728 05
0.180	0.0300	284.645 05	85.116 59
0.180	0.1200	146.923 97	71.293 30
0.180	0.1800	541.814 47	95.038 02
0.195	0.1500	290.180 01	86.710 52
0.210	0.1200	220.975 99	84.371 90
0.240	0.1200	629.175 09	111.625 89
0.270	0.0975	1457.971 62	154.650 08
0.300	0.0600	1120.215 70	201.912 44

TABLE II. Linearly polarized three-photon transition amplitudes for hydrogen atom in the presence of Debye plasmas with Debye length of 7 as a function of incident photon frequencies in atomic unit.

ω_1	ω_2	$D^{(3)L}_{1s\text{-}p\text{-}s\text{-}2p}$	$D^{(3)L}_{1s\text{-}p\text{-}d\text{-}2p}$
0.003 47	0.066 00	−6260.761 52	337.980 35
0.052 10	0.066 00	386.053 13	142.378 95
0.148 20	0.118 10	180.904 97	89.140 26
0.162 10	0.162 10	575.237 41	122.806 82
0.192 20	0.088 00	241.182 66	105.809 86
0.192 20	0.118 10	360.419 88	117.084 89
0.206 10	0.044 00	336.276 06	121.305 19
0.206 10	0.088 00	297.733 18	117.877 47
0.206 10	0.118 10	633.859 87	136.387 04
0.222 30	0.030 10	523.573 41	143.949 79
0.236 20	0.030 10	591.852 22	161.976 51
0.310 30	0.002 32	−7616.260 06	783.915 16

$$M = \frac{1}{6}\sum_{n,n'} C_{nn'}\left[\sum_{i=1}^{6}\frac{1}{D_i}\right]. \tag{32}$$

The denominators D_i $(i=1,2,\ldots,6)$ are given below,

$$\begin{aligned}
D_1 &= (\Delta_{n'} - \hbar\omega_1)(\Delta_n - \hbar\omega_1 - \hbar\omega_2),\\
D_2 &= (\Delta_{n'} - \hbar\omega_1)(\Delta_n - \Delta E + \hbar\omega_2),\\
D_3 &= (\Delta_{n'} - \hbar\omega_2)(\Delta_n - \Delta E + \hbar\omega_1),\\
D_4 &= (\Delta_{n'} - \hbar\omega_2)(\Delta_n - \hbar\omega_2 - \hbar\omega_1),\\
D_5 &= (\Delta_{n'} - \Delta E + \hbar\omega_1 + \hbar\omega_2)(\Delta_n - \Delta E + \hbar\omega_2),\\
D_6 &= (\Delta_{n'} - \Delta E + \hbar\omega_1 + \hbar\omega_2)(\Delta_n - \Delta E + \hbar\omega_1),
\end{aligned} \tag{33}$$

where $\Delta_n=E_n-E_g$ and $\Delta_{n'}=E_{n'}-E_g$. The six conditions of resonance, i.e., where the denominators become close to zero (need not be zero) are presented below,

$$\begin{aligned}
&\hbar\omega_1 \simeq \Delta_{n'}, \quad \hbar\omega_2 \simeq \Delta_{n'}, \quad \hbar\omega_1 + \hbar\omega_2 \simeq \Delta E - \Delta_{n'},\\
&\hbar\omega_1 \simeq \Delta E - \Delta_n, \quad \hbar\omega_2 \simeq \Delta E - \Delta_n, \quad \hbar\omega_1 + \hbar\omega_2 \simeq \Delta_n,
\end{aligned} \tag{34}$$

we observe resonance enhancement when Δ_n and $\Delta_{n'}$ belong to the interval $(0,\Delta E)$. We notice that for s-p-s-p channel $\Delta_{1'}$ belongs to the interval $(0,\Delta E)$ for free hydrogen atom (it should be noted that $\Delta_{1'}$ is very close to ΔE, the difference is less than 10^{-30}) and $\Delta_{1'}$ and Δ_2 belong to $(0,\Delta E)$ when $\lambda_D=7$. The values of ΔE for $\lambda_D=\infty$ and $\lambda_D=7$ are different. It follows from the set of inequalities (34), there are three resonances for free hydrogen atom [satisfy three conditions in Eq. (34)] and six resonances for $\lambda_D=7$ [satisfy six conditions in Eq. (34)]. In the case of s-p-d-p channel only $\Delta_{1'}$ belongs to the interval $(0,\Delta E)$ for both cases, free hydrogen and in the presence of Debye plasmas with Debye length of 7. Therefore we get only three resonances for s-p-d-p channel in both cases.

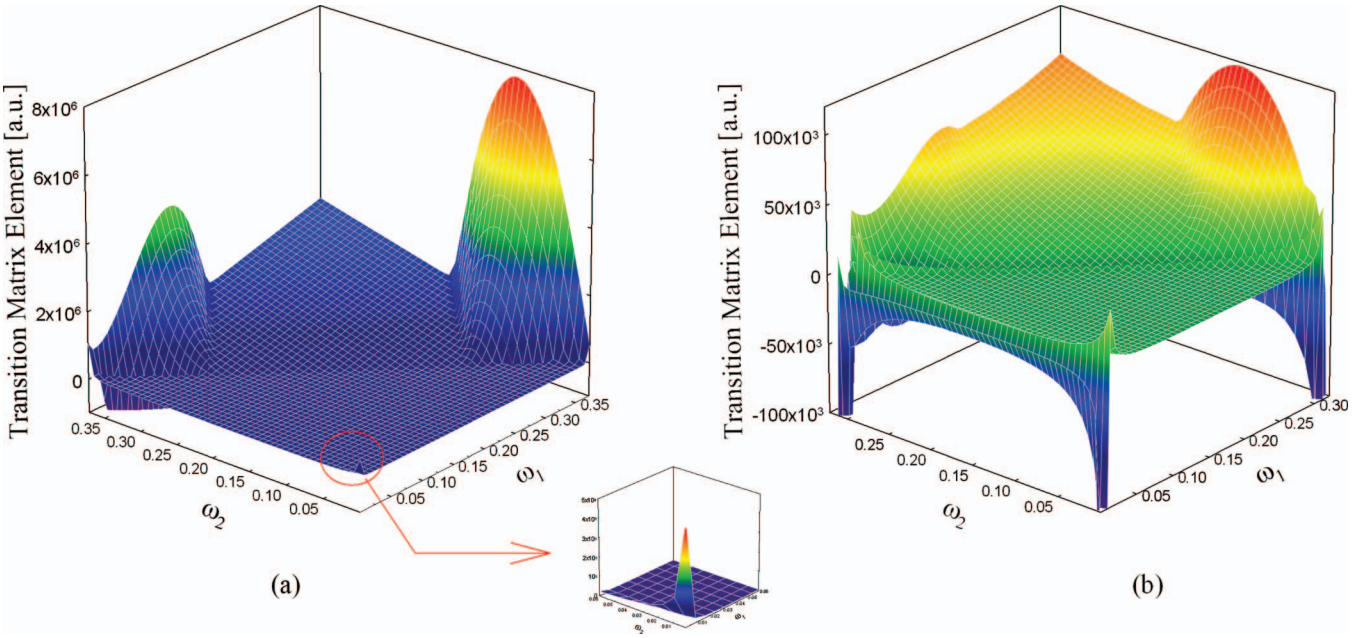

FIG. 9. (Color) Transition matrix elements $D_{1s\text{-}2p}^{(3)C}$ as a function of photon frequencies ω_1 and ω_2 for $1s$-$2p$ transition in (a) free hydrogen atom and (b) hydrogen atom embedded in Debye plasma with Debye length of 5. *C* indicates circularly polarized photons.

2. Three-photon transparency

Transparency is the material property of allowing light to pass through, i.e., photons are not absorbed. In case of three-photon transparency some values of M, the transition matrix element, in Eq. (32) are negative. Thus the condition of transparency will be evaluated if we can determine the condition of $M<0$. It is happened when any one of D_i $(i=1,2,\ldots,6)$ in expressions (33) is negative near a resonance point, the corresponding range of $\hbar\omega_1$ and $\hbar\omega_2$, the energies of two photons, are given below,

$$\begin{aligned}
&\hbar\omega >_c \Delta_{n'}, \quad \hbar\omega' >_c \Delta E - \Delta_n,\\
&\hbar\omega <_c \Delta_{n'}, \quad \hbar\omega' <_c \Delta E - \Delta_n,\\
&\hbar\omega >_c \Delta_{n'}, \quad \hbar\omega + \hbar\omega' <_c \Delta_n,\\
&\hbar\omega <_c \Delta_{n'}, \quad \hbar\omega + \hbar\omega' >_c \Delta_n,\\
&\hbar\omega + \hbar\omega' >_c \Delta E - \Delta_{n'}, \quad \hbar\omega' <_c \Delta E - \Delta_n,\\
&\hbar\omega + \hbar\omega' <_c \Delta E - \Delta_{n'}, \quad \hbar\omega' >_c \Delta E - \Delta_n.
\end{aligned} \tag{35}$$

In expressions (35) ω and ω' are either ω_1 or ω_2 but for a particular range, as example (35a), when we consider $\omega=\omega_1$, ω' must be ω_2. $x>_c y$ indicates that x is greater than and close to y. The energy conservation relation implies one more condition $0<\hbar\omega_1+\hbar\omega_2<\Delta E$. The three-photon transparency appears when Δ_n or $\Delta_{n'}$ or both (for one or more values of n and n') belong into the interval $(0, \Delta E-\delta]$, where δ should be greater than minimum possible values of photon energy. For $\lambda_D=\infty$ (in both the channel calculation) and $\lambda_D=7$ (in s-p-d-p channel computation), we find $\Delta E-\delta<\Delta_{1'}<\Delta E$ (in the present calculation δ is less than 10^{-30}) and Δ_n, $\Delta_{n'}>\Delta E$ for all n and $n'\geqslant 2$ which does not satisfy the condition of transparency. Numerically we observe $0<\Delta_2<\Delta_{1'}<\Delta E-\delta$ for s-p-s-p channel, which satisfies the condition of transparency at $\lambda_D=7$.

B. Circularly polarized photons

Figure 9(a) shows three-photon $1s$-$2p$ transition amplitudes for free hydrogen atom as a function of ω_1 and ω_2, the frequencies of two photons. There is no three-photon transparency for free hydrogen, although resonance enhancements are present. In the presence of Debye plasma field with Debye length of 5, we observe three-photon transparency [shown in Fig. 9(b)] and resonance enhancement for $1s$-$2p$ transition. No three-photon transparency occurs from $\lambda_D=\infty$ (free hydrogen atom) up to $\lambda_D=10$. For $\lambda_D=9$, transparency is started to appear. Three-photon transparency is observed for $\lambda_D=9,8,\ldots,5$ (integer value), when $\lambda_D\leqslant 4$ the bound state $2p$ is disappeared. Figure 9(a) shows three resonance peaks; the magnitudes of the peaks are different, one large, one medium, and the last one is very small [inset of Fig. 9(a)]. In Fig. 9(b), seven resonances have been found with different magnitudes. In the resonance section, we shall discuss the phenomena briefly. In Figs. 10(a) and 10(b), we present the partial transition matrix element due to the s-p-s-p channel for $\lambda_D=\infty$ and $\lambda_D=5$, respectively. In the case of s-p-d-p channel transition amplitude, there are no three-photon transparency for both cases, $\lambda_D=\infty$ [Fig. 10(c)] and $\lambda_D=5$ [Fig. 10(d)]. We observe only three resonance peaks in two cases, Figs. 10(c) and 10(d). Those figures show that the partial transition amplitudes of s-p-s-p channel dominate that of s-p-d-p channel. Some numerical data of the transition matrix elements are presented in Table III.

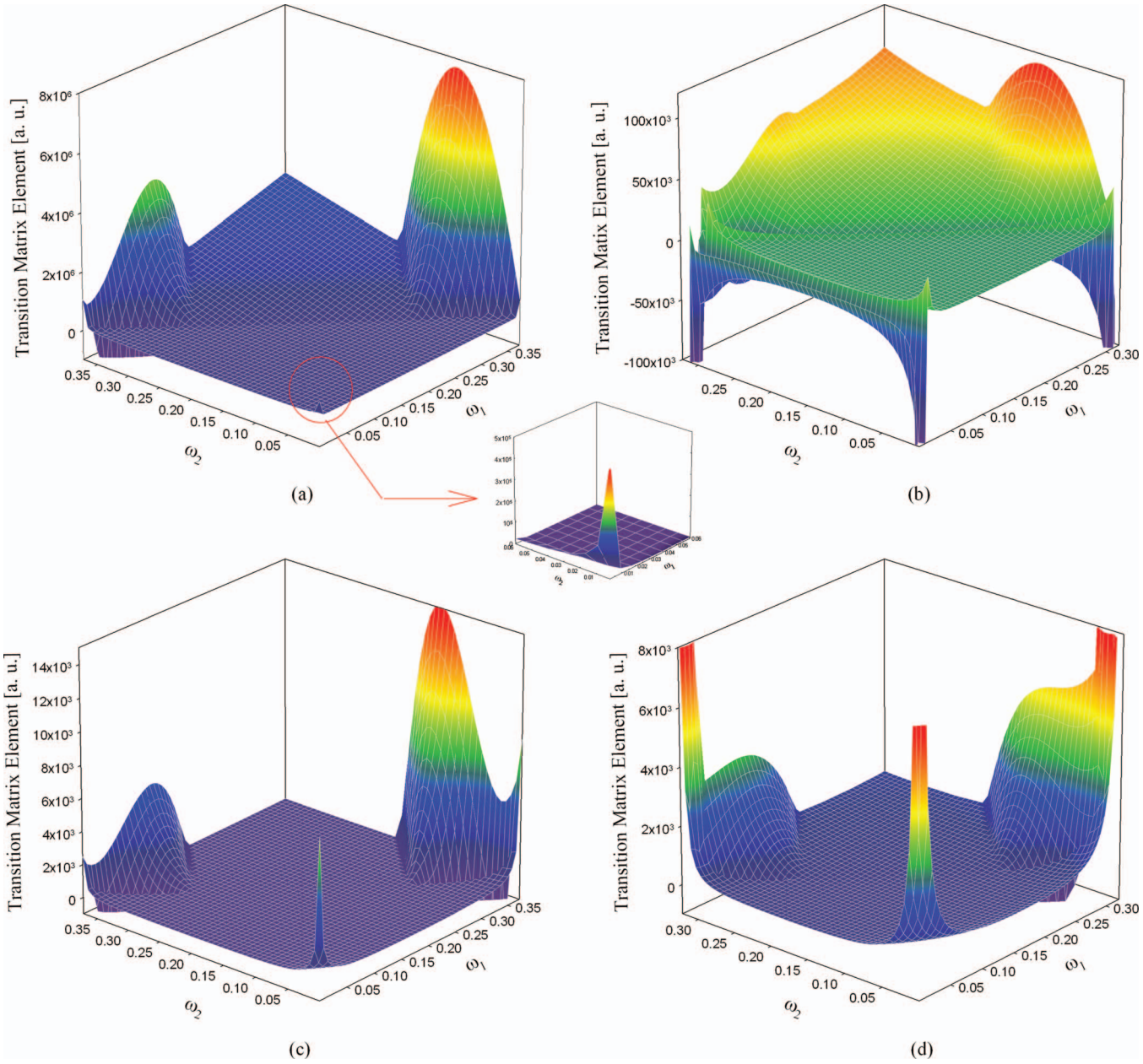

FIG. 10. (Color) Partial transition matrix elements as a function of photon frequencies ω_1 and ω_2 (a) $D^{(3)C}_{1s\text{-}p\text{-}s\text{-}2p}$ for $1s$-$2p$ transition in free hydrogen atom, (b) $D^{(3)C}_{1s\text{-}p\text{-}s\text{-}2p}$ for $1s$-$2p$ transition in hydrogen atom embedded in Debye plasma with Debye length of 5, (c) $D^{(3)C}_{1s\text{-}p\text{-}d\text{-}2p}$ for $1s$-$2p$ transition in free hydrogen atom, (d) $D^{(3)C}_{1s\text{-}p\text{-}d\text{-}2p}$ for $1s$-$2p$ transition in hydrogen atom embedded in Debye plasma with Debye length of 5. C indicates circularly polarized photons.

TABLE III. Circularly polarized three-photon transition amplitudes as a function of incident photon frequencies in atomic unit.

		$D^{(3)C}_{1s\text{-}p\text{-}s\text{-}2p}$		$D^{(3)C}_{1s\text{-}p\text{-}d\text{-}2p}$	
ω_1	ω_2	$\lambda_D=\infty$	$\lambda_D=5$	$\lambda_D=\infty$	$\lambda_D=5$
0.1	0.1	118.181	196.848	50.533	73.272
0.1	0.2	214.619	1 315.770	35.77	69.219
0.2	0.1	153.126	1 119.822	54.475	109.904
0.005	0.3	4383.990	−12 773.338	63.290	621.964

1. Resonance enhancement

The process is said to be resonant whenever an intermediate state of the target spectrum is closely reached from the initial state by absorption of one or two photons. In the present section, we discuss about resonance enhancement for individual channel. For s-p-s-p channel, from Eqs. (15), (16), and (18) we get that the transition matrix elements $D^{(3)C}_{1s\text{-}p\text{-}s\text{-}2p}$ are the sum of four different factions,

$$D^{(3)C}_{1s\text{-}p\text{-}s\text{-}2p} = \frac{1}{12\sqrt{3}} \sum_{n,n'} C_{nn'} \left[\frac{1}{D_1} + \frac{1}{D_2} + \frac{1}{D_3} + \frac{1}{D_4} \right]. \quad (36)$$

The denominators of those factions are given below,

$$D_1 = (\Delta_{n'} - \hbar\omega_1)(\Delta_n - \hbar\omega_1 - \hbar\omega_2),$$

$$D_2 = (\Delta_{n'} - \hbar\omega_3)(\Delta_n - \hbar\omega_3 - \hbar\omega_2), \tag{37}$$

$$D_3 = (\Delta_{n'} - \hbar\omega_2)(\Delta_n - \hbar\omega_2 - \hbar\omega_1),$$

$$D_4 = (\Delta_{n'} - \hbar\omega_2)(\Delta_n - \hbar\omega_2 - \hbar\omega_3),$$

where $\Delta_n = E_n - E_g$ and $\Delta_{n'} = E_{n'} - E_g$. Using the energy conservation relation, the above set of divisors reduces to

$$D_1 = (\Delta_{n'} - \hbar\omega_1)(\Delta_n - \hbar\omega_1 - \hbar\omega_2),$$

$$D_2 = (\Delta_{n'} - \Delta E + \hbar\omega_1 + \hbar\omega_2)(\Delta_n - \Delta E + \hbar\omega_1), \tag{38}$$

$$D_3 = (\Delta_{n'} - \hbar\omega_2)(\Delta_n - \hbar\omega_1 - \hbar\omega_2),$$

$$D_4 = (\Delta_{n'} - \hbar\omega_2)(\Delta_n - \Delta E + \hbar\omega_1).$$

Mathematically the condition of resonances, i.e., where the denominators become close to zero (need not be zero) are given below,

$$\hbar\omega_1 \cong \Delta_{n'}, \quad \hbar\omega_1 \cong \Delta E - \Delta_n, \quad \hbar\omega_2 \cong \Delta_{n'},$$

$$\hbar\omega_1 + \hbar\omega_2 \cong \Delta_n, \quad \hbar\omega_1 + \hbar\omega_2 \cong \Delta E - \Delta_{n'}, \tag{39}$$

where Δ_n and $\Delta_{n'}$ belong to the interval $(0, \Delta E)$. If Δ_n and $\Delta_{n'}$ belong to the interval $(0, \Delta E)$ for $n = 1, 2, \ldots, i$ and $n' = 1, 2, \ldots, j$; the total number of resonance surfaces is $2i + 3j$, provided all the elements of the pairs $(\Delta_{n'}, \Delta E - \Delta_n)$ and $(\Delta_n, \Delta E - \Delta_{n'})$ are distinct. If $\Delta_{m'}$ and $\Delta E - \Delta_m$ are the same for $m' \leqslant j$, $m \leqslant i$, the two resonance surfaces corresponding $\hbar\omega_1 \cong \Delta_{m'}$ and $\hbar\omega_1 \cong \Delta E - \Delta_m$ coincide. Similar things happen when Δ_k and $\Delta E - \Delta_{k'}$ are the same for $k \leqslant i$, $k' \leqslant j$. Numerically it is observed that $\Delta_{1'}$ belongs to the interval $(0, \Delta E)$ for plasma free situation. Therefore, there are three resonance surfaces [Fig. 10(a)] for plasma-free partial transition, followed by *s-p-s-p* channel. For $\lambda_D = 5$, we observe that Δ_1, Δ_2, and $\Delta_{1'}$ belong to the interval $(0, \Delta E)$ which implies seven resonance surfaces. Here it should be noted that the value of ΔE is dissimilar for different λ_D. Considering only equal sign, the set of Eq. (39) reduces to a branch of straight line equations.

Using the similar procedure, we get the condition of resonances for *s-p-d-p* channel as follows:

$$\hbar\omega_1 \cong \Delta_{n'}, \quad \hbar\omega_1 \cong \Delta E - \Delta_n, \quad \hbar\omega_2 \cong \Delta_{n'},$$

$$\hbar\omega_2 \cong \Delta E - \Delta_n, \quad \hbar\omega_1 + \hbar\omega_2 \cong \Delta_n, \quad \hbar\omega_1 + \hbar\omega_2 \cong \Delta E - \Delta_{n'}, \tag{40}$$

where Δ_n and $\Delta_{n'}$ belong to the interval $(0, \Delta E)$. If Δ_n and $\Delta_{n'}$ belong to the interval $(0, \Delta E)$ for $n = 1, 2, \ldots, i$ and $n' = 1, 2, \ldots, j$; the total number of resonance surfaces is $3(i+j)$, provided all the elements of the pairs $(\Delta_{n'}, \Delta E - \Delta_n)$ and $(\Delta_n, \Delta E - \Delta_{n'})$ are distinct. If $\Delta_{m'}$ and $\Delta E - \Delta_m$ are the same for $m' \leqslant j$, $m \leqslant i$, we observe two resonance surfaces instead of four resonance surfaces corresponding $\hbar\omega_1 \cong \Delta_{m'}$, $\hbar\omega_1 \cong \Delta E - \Delta_m$, $\hbar\omega_2 \cong \Delta_{m'}$, and $\hbar\omega_2 \cong \Delta E - \Delta_m$. If Δ_k and $\Delta E - \Delta_{k'}$ are the same for $k \leqslant i$, $k' \leqslant j$, the two resonance surfaces corresponding $\hbar\omega_1 + \hbar\omega_2 \cong \Delta_k$ and $\hbar\omega_1 + \hbar\omega_2 \cong \Delta E - \Delta_{k'}$ turn into one surface. Numerically it is observed that $\Delta_{1'}$ belongs to the interval $(0, \Delta E)$ for plasma-free case and for $\lambda_D = 5$. Therefore, there are three resonance surfaces for both the cases.

2. Three-photon transparency

Transparency is the material property of allowing light to pass through, i.e., photons are not absorbed. The detailed expression of partial transition matrix element $D^{(3)C}_{1s\text{-}p\text{-}s\text{-}2p}$ for *s-p-s-p* channel, where three-photon transparency occurs for $\lambda_D = 9, 8, \ldots, 5$, has been already presented in Eq. (36). In the case of three-photon transparency some values of $D^{(3)C}_{1s\text{-}p\text{-}s\text{-}2p}$ are negative. Thus the condition of transparency will be evaluated if we can determine the condition of $D^{(3)C}_{1s\text{-}p\text{-}s\text{-}2p} < 0$. From Eq. (36) we can easily see that $D^{(3)C}_{1s\text{-}p\text{-}s\text{-}2p} < 0$, when denominator (denominators) becomes (become) negative near a resonance point. From the set of Eq. (37), we obtain eight stipulations for which the denominators D_1, D_2, D_3, and D_4 are negative, respectively. The energy conservation relation implies one more condition $0 < \hbar\omega_1 + \hbar\omega_2 < \Delta E$. The three-photon transparency appears when Δ_n or $\Delta_{n'}$ or both (for one or more values of n and n') belong into the interval $(0, \Delta E - \delta]$, where δ is greater than minimum possible values of photon energy. For $\lambda_D = \infty$, we find $\Delta E - \delta < \Delta_{1'} < \Delta E$ and Δ_n, $\Delta_{n'} > \Delta E$ for all n and $n' \geqslant 2$ which does not satisfy the condition of transparency. Numerically we observe $0 < \Delta_2 < \Delta_{1'} < \Delta E - \delta$ which satisfies the condition of transparency at $\lambda_D = 5$. This type of phenomena happen because due to Debye plasma environments energy levels of hydrogen atom are shifted.

IV. CONCLUSION

The transition matrix elements are presented in the context for three-color three-photon $1s$-$2p$ transition in hydrogen atom, free and in the presence of Debye plasma field. The three-photon transparency appears when hydrogen atom embedded in weakly coupled Debye plasmas. Here, we consider that three photons are linearly polarized and circularly polarized. Present results show that Debye plasma environments have a considerable effect on the three-photon bound-bound transitions.

The dynamic motion of the plasma electrons has to be considered in order to investigation the plasma screening effect on hydrogen atom can be considered qualitatively by the introduction of the plasma dielectric function.[32] The effects may be very important for high density plasma, but for low density plasma the effect can be neglected. The static plasma screening formula obtained by the Debye–Huckel model overestimates the plasma screening effects on the hydrogen atom in dense plasma. The static screening result presented here is subject to the condition that the plasma is a thermodynamically equilibrium plasma and neglect the contributions from ions in plasma since electrons provide more effective shielding than ions. In the static plasma screening, we observe that the two-photon transition amplitude is mainly determined by the Debye length, which in turn is determined

by the plasma temperature and density. With increase in plasma density at a given temperature, the Debye length decreases, and thus the effect from plasma temperature and density cannot be neglected.

ACKNOWLEDGMENTS

The authors would like to thankfully acknowledge financial support by the National Science Council of Taiwan, ROC.

[1] *Advances in Multi-Photon Processes and Spectroscopy*, edited by S. H. Lin, A. A. Villaeys, and Y. Fujimura (World Scientific, Singapore, 2004), Vol. 16.
[2] G. J. Hatton, N. F. Lane, and J. C. Weisheit, J. Phys. B **14**, 4879 (1981).
[3] N. C. Deb and N. C. Sil, J. Phys. B **17**, 3587 (1984).
[4] J. C. Weisheit, Adv. At. Mol. Phys. **25**, 101 (1988).
[5] R. K. Janev, L. P. Presnyakov, and V. P. Shevelko, *Physics of Highly Charged Ions* (Springer-Verlag, Berlin, 1985), Chap. 3.
[6] D. Salzmann, J. Stein, I. B. Goldberg, and R. H. Pratt, Phys. Rev. A **44**, 1270 (1991).
[7] V. P. Shevelko and L. A. Vainshtein, *Atomic Physics for Hot Plasmas* (Institute of Physics, London, 1993), Chap. 1.
[8] F. A. Gutierrez and J. Diaz-Valdes, J. Phys. B **27**, 593 (1994).
[9] R. Brandenburg, J. Schweinzer, S. Fiedler, F. Aumayr, and H. P. Winter, Plasma Phys. Controlled Fusion **41**, 471 (1999).
[10] L. B. Zhao and Y. K. Ho, Phys. Plasmas **11**, 1695 (2004).
[11] W. Hong and Y. D. Jung, Phys. Plasmas **3**, 2457 (1996).
[12] Y. D. Jung, Physica B **5**, 3432 (1993); Phys. Plasmas **2**, 332 (1995); **2**, 987 (1995); **5**, 3781 (1998); **5**, 4456 (1998).
[13] J. S. Yoon and Y. D. Jung, Phys. Plasmas **3**, 3291 (1996).
[14] U. Gupta and A. K. Rajagopal, Phys. Rep. **87**, 259 (1982).
[15] B. L. Whitten, N. F. Lane, and J. C. Weisheit, Phys. Rev. A **29**, 945 (1984).
[16] H. Zhang, J. G. Wang, B. He, and Y. B. Qiu, Phys. Plasmas **14**, 053505 (2007).
[17] Y. Y. Qi, Y. Wu, and J. G. Wang, Phys. Plasmas **16**, 033507 (2009).
[18] Y. Y. Qi, Y. Wu, and J. G. Wang, Phys. Plasmas **16**, 023502 (2009).
[19] M. R. Flanney and E. Oks, Eur. Phys. J. D **47**, 27 (2008).
[20] L. Liu, J. G. Wang, and R. K. Janev, Phys. Rev. A **77**, 032709 (2008); **77**, 042712 (2008).
[21] M. S. Pindzola, S. D. Loch, J. Colgan, and C. J. Fontes, Phys. Rev. A **77**, 062707 (2008).
[22] C. Stubbins, Phys. Rev. A **48**, 220 (1993).
[23] P. M. Bellan, Phys. Plasmas **11**, 3368 (2004).
[24] A. C. H. Yu and Y. K. Ho, Phys. Plasmas **12**, 043302 (2005).
[25] S. Sahoo and Y. K. Ho, Phys. Plasmas **13**, 063301 (2006).
[26] S. Kar and Y. K. Ho, Phys. Plasmas **15**, 013301 (2008).
[27] S. Paul and Y. K. Ho, Phys. Plasmas **15**, 073301 (2008).
[28] S. Paul and Y. K. Ho, Phys. Rev. A **78**, 042711 (2008).
[29] S. Paul and Y. K. Ho, Phys. Rev. A **79**, 032714 (2009).
[30] S. Paul and Y. K. Ho, Phys. Plasmas **16**, 063302 (2009).
[31] R. B. Thayyullathil, R. Radhakrishnan, and M. Seema, J. Phys. A **36**, 8473 (2003).
[32] Y. D. Jung, Phys. Rev. E **55**, 3369 (1997);C. G. Kim and Y. D. Jung, Phys. Plasmas **5**, 3493 (1998).